proper consideration must however by given to the added weight, reliability and cost factors.

The data just presented covers Engine "A" with a relatively low tip speed fan. The next major step in the NASA/GE experimental Quiet Engine Program is to evaluate an engine incorporating Fan "C" which is representative of a high speed fan. Such an engine offers the advantage of having shorter length and fewer components, both of which permit important improvements in engine weight and engine cost. It is expected that the acoustic investigation of the Engine "C" technology demonstrator will be pursued into the Spring of 1973. At that time comparable data will have been obtained on both "A" and "C" technology demonstrators and tradeoff studies will be performed to evaluate their relative merits acoustically and in terms of direct operating costs on a number of airplane applications.

References

[1]Sanders, N. D., "Some Results of Recent Research on Fan and Jet Noise," Paper 70-WA/GT15, ASME. Nov., 1970.

[2]Kohn, A. O., "Noise Considerations in High Bypass Ratio Fan Engine Design," Paper 70-WA/GT14, ASME. Nov., 1970.

[3]*Federal Aviation Regulations, Noise Standards, Aircraft Type Certification,* Vol. III, Pt. 36, Federal Aviation Agency, Washington, D. C., Dec. 1, 1969.

[4]Bishop, D. E. and Simpson, M. A., "Noise Exposure Forecast Contours for 1967, 1970 and 1975 Operations at Selected Airports," Rept. 70-8, 1970, Federal Aviation Agency, Washington, D. C.

[5]"The Integration of Quiet Engines with Subsonic Transport Aircrafts," Rept. DAC-68256, June 24, 1968, McDonnell Douglas, Long Beach, Cal.; also NASA CR-72548, Aug., 1969.

Measurements of the Boundary-Layer Growth in Annular Diffusers

Stanley J. Stevens*
University of Technology, Loughborough, England
and
Peter Fry†
Rolls-Royce (1971) Ltd., Derby, England

Low speed tests have been carried out on two-optimum straight walled, annular diffusers. One diffuser had a uniform diameter center body, the other an expanding diameter center body (divergence angle 40°). Curved passages of constant flow path area were situated up- and downstream of the expanding center body diffuser. Measurements were made of the pressure recovery, mean total pressure loss, and the growth of the boundary layers in terms of the mean velocity profile and turbulence structure. The rate of growth of the shape parameters was found to be significantly greater along the outer wall, this effect is attributed to the distortion caused by flow curvature at inlet which is then accentuated by the adverse pressure gradient. Whereas the pressure recovery of the two diffusing systems was comparable, a significant increase in losses occurred in the expanding center body diffuser, due to the higher turbulence level of the flow from the curved inlet passage increasing the energy dissipation.

Nomenclature

A = area of cross section
AR = area ratio
B = blocked area fraction, $1 - 1/A_0 \int_0^A (u/U) dA$
C_f = local skin friction coefficient
$\overline{C}_p$ = pressure recovery coefficient based on $\rho \bar{u}_1^2/2$
$\overline{C}_p{}^*$ = the locus of maximum pressure recovery at prescribed nondimensional length
$\overline{C}_{p_{\text{comp}}}$ = the pressure recovery associated with a component in a duct system
D = diameter of cross section
D_h = hydraulic mean diameter
H = shape parameter
L = average diffuser wall length
L_e = length of approach pipe upstream of diffuser
N = diffuser axial length
P = static pressure
P_T = total pressure
R_m = radius of the point of maximum velocity
ΔR = annulus height
u = local velocity in x direction
$\bar{u}$ = mean velocity in cross section $\int_0^A u dA/A$
u_τ = friction velocity, $(\tau_w/\rho)^{1/2}$
$(\langle u'^2 \rangle)^{1/2}$, $(\langle v'^2 \rangle)^{1/2}$ = rms velocity fluctuation in x and y directions, respectively
$\langle -\rho u'v' \rangle$ = Reynolds shear stress
U = maximum velocity in cross section
x = distance along the mean flow line from diffuser inlet
y = distance perpendicular to wall
α = velocity profile energy coefficient $\int_0^A (u/\bar{u})^3 dA/A$
γ = pressure gradient parameter $(\nu/\rho u_\tau{}^3) dP/dx$
δ_o, δ_i = boundary-layer thickness on outer and inner walls, respectively
$\delta_o{}^*, \delta_i{}^*$ = displacement thickness of boundary layer on outer and inner walls, respectively, $\delta_o{}^* = \int_0^{\delta o} (1 - u/U)(R/R_o) dy$, $\delta_i{}^* = \int_0^{\delta i} (1 - u/U)(R/R_i) dy$
θ_o, θ_i = momentum thickness of boundary layer on outer and inner walls, respectively, $\theta_o = \int_0^{\delta o} (1 - u/U)(u/U)(R/R_o) dy$, $\theta_i = \int_0^{\delta i} (1 - u/U)(u/U)(R/R_i) dy$
λ = loss coefficient, $\Delta P_T/(\rho \bar{u}_1^2/2)$
ν = kinematic viscosity
ρ = fluid density
τ = shear stress
ϕ = diffuser wall angle
$'$ = fluctuation quantity
$\langle\ \rangle$ = time average

Presented as Paper 72-86 at the AIAA 10th Aerospace Sciences Meeting, San Diego, Calif., January 17-19, 1972; submitted May 5, 1972; revision received October 30, 1972. The tests on the uniform center body diffuser were supported by S. R. C. Grant B/SR/3734.

Index categories: Aircraft Powerplant Design and Installation; Boundary Layers and Convective Heat Transfer—Turbulent.

*Senior Lecturer, Department of Transport Technology.
†Senior Combustion Engineer.

Subscripts

1 = diffuser inlet
i = inner wall
o = outer wall
m = position of maximum velocity

Introduction

MANY diffuser applications, particularly in gas turbines, involve diffusion in an annular passage. At the large values of compressor exit hub/tip ratio the flow in a symmetrical annular diffuser is approximately two-dimensional and therefore many designs have been based on the two-dimensional tests of Kline et al.[1] However annular diffuser design has now been brought on to a much firmer basis by Sovran and Klomp[2] who carried out a comprehensive investigation on over one hundred different diffuser geometries. The large majority of the diffusers tested had expanding center bodies and the value of inlet hub/tip ratio $(R_i/R_o)_1$ was 0.55 or 0.70. These tests were carried out with a thin inlet boundary layer, and the diffusers had a free discharge. The optimum performance at a fixed nondimensional length $L/\Delta R_1$ measured in terms of the pressure recovery coefficient was found to occur at an area ratio approximately independent of the combination of wall angles and hub/tip ratio employed. The outlet velocity profiles were not measured and therefore only approximate values of the total pressure loss coefficient can be obtained.

Hoadley[3] has investigated the growth of the boundary layers in a diffuser having a constant diameter center body and although the influence of inlet swirl was the primary objective in this work some tests were carried out with axial flow at inlet. Under these conditions separation on the outer wall was encountered however, useful data was obtained on the growth of the boundary layer along the center body.

That the growth of the boundary layers is crucial in determining the performance of a diffuser has been ably demonstrated by Cocanower et al[4] and Imbach.[5] They show that for "boundary layer" types of inlet nonuniformity the pressure recovery and total pressure loss can be predicted, within the limits of engineering accuracy, for two-dimensional and axially-symmetric diffusers by the use of simple integral calculation techniques. At present no reliable method exists to calculate through a region of separated flow and therefore such calculations are restricted to diffusers that are free from stalling, furthermore it is assumed that a potential core exists over the length of the diffuser. However many practical diffuser systems operate in or near the region of transitory stalling, also in certain applications, typically prior to a gas turbine combustion system, diffusion may occur after the air has been turned through an angle of up to 40°. Furthermore the velocity profile and turbulence structure of the flow presented to the diffuser by the compressor may be far removed from the thin inlet boundary layer condition frequently used in diffuser research.

The influence of upstream and downstream bends has been neglected in the literature and there is therefore a need for detailed measurements of the boundary layer growth in annular diffusing systems which can serve as a basis for analytical studies and lead to a better understanding of the flow behaviour. Such data should be free from significant three-dimensional effects, and be obtained for representative pressure gradiants and inlet conditions.

Tests were therefore carried out on an expanding center body diffuser, operating near to the optimum $\bar{C}_p$* line, to: 1) investigate the growth of the boudary layers, 2) assess the influence of the inlet and outlet bends. The results are compared with those obtained from an optimum diffuser having a uniform diameter center body.[6]

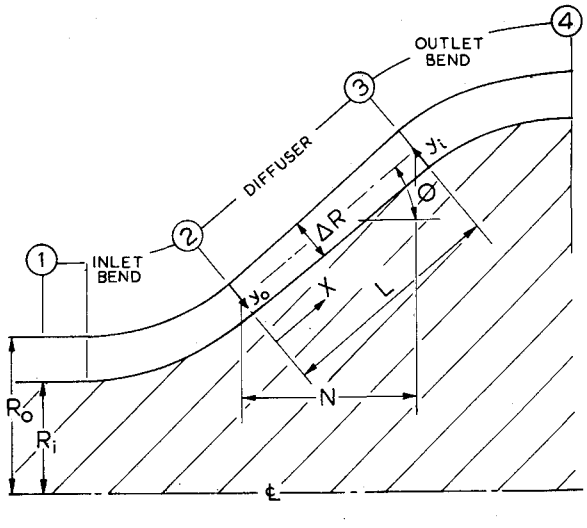

Fig. 1 Geometric characteristics of annular diffusers.

Test Facility

The test facility is shown in Fig. 2. The entry length, diffuser, and settling length were mounted vertically, the advantage of this arrangement was that as all the inner tubes were spigotted together they could be positioned simply by three struts in the entry flare, the weight of the tubes was supported by two rods at the end of the settling length. In this way the influence of entry length supports was reduced to a minimum. Two diffuser geometries were selected: 1) A minimum length diffuser ($\bar{C}_p$*) which had a center body of uniform diameter, 2) An expanding center body diffuser with a mean divergence half-angle of 40°.

The geometry of the diffusers is detailed in Table 1. Curved passages of constant flow path area were situated up- and downstream of the expanding center body diffuser. Whereas both diffusers had a common area ratio of 2.0 the nondimensional length of the expanding center body diffuser was increased from 5.0 to 6.2 to compensate for the inferior velocity profile presented to the diffuser by the inlet bend.

Air was drawn from the laboratory through a bell-shaped inlet into an annular entry length some $50L_e/D_{h_1}$ long. Transition on the bell-mouth and forebody of the center body was stabilised by trip wires. The entry length was constructed in perspex to a very high standard of accuracy (typically 10.000 in. ± 0.003 in. diam over a length of 30 in.).

An almost constant dynamic pressure was maintained in the center of the annulus at a position 3.0 in. upstream of the exit of the entry length. This corresponded to a velocity of 140 fps, and a Reynolds number based on inlet hydraulic diameter of 1.50×10^5.

Table 1 Diffuser geometry

	Uniform center body diffuser	Expanding center body diffuser
D_{o1} in.	12.0	12.0
D_{i1} in.	10.0	10.0
ϕ_o°	10.0	41.0
ϕ_i°	0	39.0
ΔR_2 in.	...	0.816
$L/\Delta R_1$	5.0	...
$L/\Delta R_2$	...	6.2
AR	2.0	2.0

Static pressure measurements were made at positions near to the exit of the entry length, and along the length of the inlet bend, diffuser, outlet bend/settling length. At each position three tappings were made equally spaced around the surface of the inner and outer walls. Total pressure traverses were carried out at three circumferential positions, 120° apart, for each of the nine stations along the length of the diffuser. The flattened total pressure tube had a wall thickness of 0.005 in., and an opening of 0.040 in., by 0.015 in. The traverses were carried out normal to the walls of the tubes, and all pressures were recorded on Betz projection manometers.

The velocity profiles were calculated on the assumption that the static pressure, along each traverse, was the same as that measured at the wall. The only exception to this technique was at inlet to the expanding center body diffuser where the velocity profile was obtained using the measured static pressure variation across the annulus. The pressure variation was obtained using a wedge probe developed by Girerd and Guienne.[7] Whereas an allowance was made for the displacement of the effective center of the pitot probe no corrections were applied to take account of the effects of turbulence. Considerable uncertainty surrounds the estimation of errors in pitot tube measurements of mean velocity when the local turbulence level is high.[8] Nonetheless the local velocities near the wall may be approximately 20% too high as the flow approaches near separating conditions. Velocity profiles taken at the three circumferential locations exhibited excellent symmetry of flow, except close to diffuser exit, and the integrated mass flows at all other positions were within 1.5% of the inlet value. Wool tuft investigations indicated that on the outer wall at exit of both diffusers intermittent transitory stalling was taking place.

The distribution of u', v', w', $\langle u'v' \rangle$ and $\langle u'w' \rangle$, at a number of positions along the length of the diffuser was obtained from measurements taken with a DISA constant temperature anemometer. No suitable X-probe was available and therefore a 45° slant wire probe was used. The technique employed was similar to that adopted by Goldberg[9] namely, that the wire was presented at an angle of 45° to the mean direction of flow, and then turned through an angle of 180°. The probe element was mounted in a square sectioned carrier which could be placed in the u'-v' and u'-w' planes. In order to minimize contamination of the hot wires a Vokes filter was placed around the inlet flare, and at the end of each traverse the wires were inspected and cleaned if necessary. The accuracy of the turbulence measurements is difficult to quantify due to such problems as misalignment of the wire, high turbulence levels, and large vertical components of velocity as the flow approaches near separating conditions. These problems have been considered by Goldberg, and Sandborn and Liu,[10] and in the light of their work the following accuracies are suggested: early stages of diffusion 5% in $(\langle u'^2 \rangle)^{1/2}$ 10–15% in $\langle u'v' \rangle$; latter stages of diffusion 20% in $(\langle u'^2 \rangle)^{1/2}$ 20–40% in $\langle u'v' \rangle$.

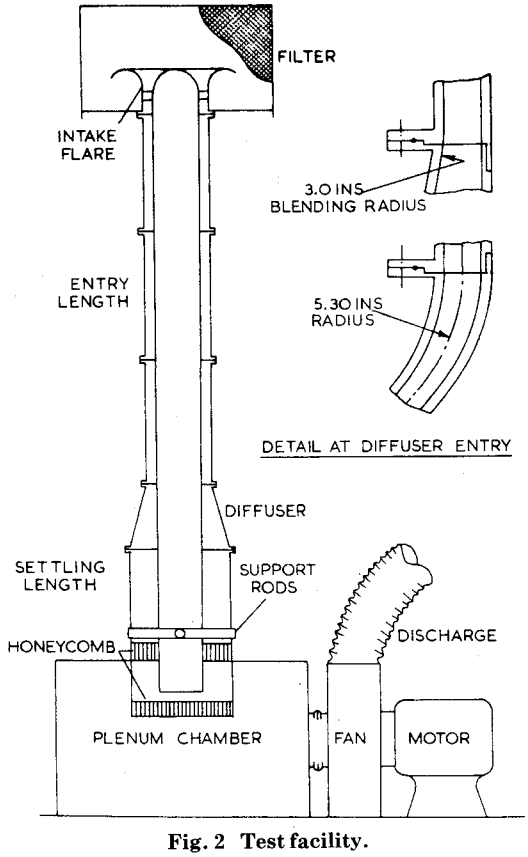

Fig. 2 Test facility.

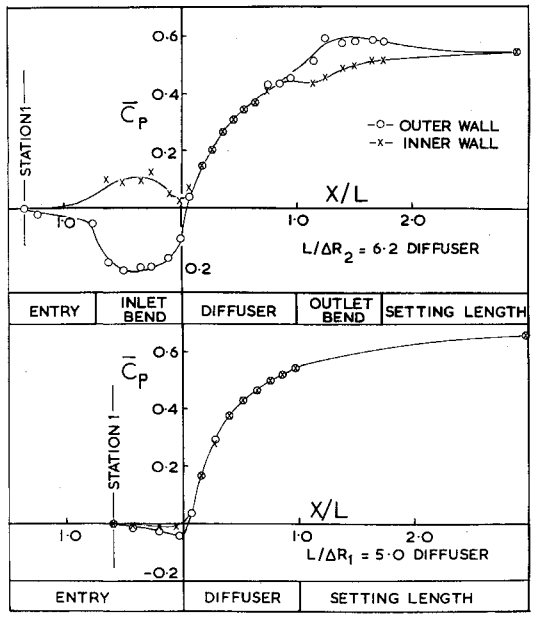

Fig. 3 Static pressure recovery.

Inlet Conditions

The velocity profile and turbulent shear stress distribution measured at station 1, 3-in. upstream of, the inlet bend of the expanding center body diffuser or the entry to the uniform center body diffuser, is shown in Figs. 4 and 6. The turbulent shear stress distribution at exit of the inlet bend of the expanding center body diffuser, station 2, is shown in Fig. 7. It will be seen that there is a considerable increase in mixing near the inner wall, and a corresponding reduction near the outer, resulting in a movement of the position of zero shear relative to the position of maximum velocity. Most of the previous experimental work on curved flow has been done in channels whose depth and breadth were of the same order of magnitude, in other words the mean flow was essentially three-dimensional in character. In this case the large hub/tip ratio means that the flow is approximately two-dimensional. The arguments put forward by Wattendorf[11] concerning the stability of flow in a curved two-dimensional channel indicate that centrifugal forces near the inner wall promote, and near to the outer wall diminish, the turbulent interchange between fluid layers. Whereas the presence of a diffuser downstream of the bend modifies the pressure distribution at exit of the bend, the results clearly confirm the predictions of Wattendorf.

Table 2 Over-all performance

	Expanding center body diffuser $L/\Delta R_2 = 6.2$			Constant center body diffuser $L/\Delta R_1 = 5.0$		
$B_1 = 0.105$	$\bar{C}_p$	$\bar{C}_{p_{comp.}}$	λ	$\bar{C}_p$	$\bar{C}_{p_{comp.}}$	λ
Entry length	-0.022^a	-0.022^a	0.022^a	-0.022^a	-0.022^a	0.022^a
Inlet bend	−0.055	−0.033	0.045	...	...	...
Diffuser	0.460	0.515	0.215	0.54	0.562	0.080
Outlet bend/ settling length	0.550	0.090	0.230	0.665	0.125	0.113

[a]Calculated values based on a friction factor of 0.0036.

Pressure Distributions

The static pressure distribution along the inner and outer walls in the two diffuser systems, with fully developed flow at inlet, is shown in Fig. 3. Because of the curvature of the flow there is a significant difference in static pressure across the annulus in the vicinity of diffuser inlet, this is particularly so in the inlet bend upstream of the expanding center body diffuser. In view of this the inlet pressure to the diffusing system is taken as the static pressure measured 3.0 in. upstream from the end of the entry length. However, over the majority of the length of the diffusers the pressures on inner and outer walls are, within experimental error, the same. Again a pressure difference exists across the annulus in the outlet bend of the expanding center body diffuser but is of smaller magnitude due to the lower dynamic pressures.

Diffuser Performance

The over-all performance of the two diffusers is summarized in Table 2. All values are calculated relative to conditions measured at station 1, 3.0 in. upstream from the end of the entry length.

In estimating the pressure at exit of the inlet bend of the expanding center body diffuser the mass-averaged value of pressure was calculated, in all other cases the arithmetic mean value was taken. The stagnation pressure at any cross section can then be expressed as $\bar{P}_T = \bar{P} + \alpha\bar{q}$, where $\bar{q} = \rho u^2/2$. The following identity can then be used to relate fluid properties at any cross section

$$\bar{P}_x - \bar{P}_1 = (\alpha_1\bar{q}_1 - \alpha_x\bar{q}_x) - (\bar{P}_{T_1} - \bar{P}_{T_x}) \qquad (1)$$

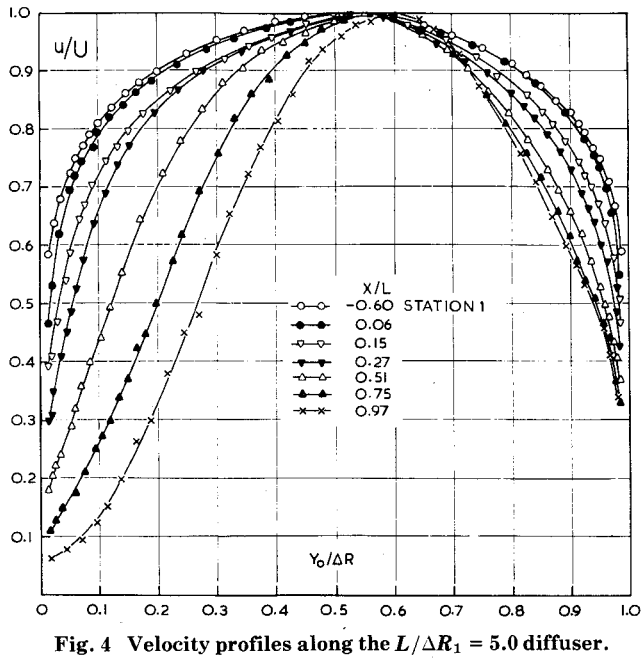

Fig. 4 Velocity profiles along the $L/\Delta R_1 = 5.0$ diffuser.

defining $\bar{C}_{p_{1-x}} = (\bar{P}_x - \bar{P}_1)/\bar{q}_1$, and continuity gives $A_1\bar{u}_1 = A_x\bar{u}_x$ hence $\bar{q}_x/\bar{q}_1 = 1/(A_x/A_1)^2 = 1/AR_x^2$ therefore

$$\bar{C}_{p_{1-x}} = [\alpha_1 - \alpha_x/AR_x^2] - \lambda_{1-x} \qquad (2)$$

where $\lambda_{1-x} = (\bar{P}_{T_1} - \bar{P}_{T_x})/\bar{q}_1$. The values of λ quoted in Table 2 have been obtained using Eq. (2), the values of α_x are given in Table 3.

It is interesting to compare the performance of the two diffusers with that predicted using the correlation due to Sovran and Klomp. In the case of the uniform center body diffuser the predicted static pressure recovery coefficient is 0.53 compared with an experimental value of 0.56. Using the blockage fraction of the flow presented by the inlet bend to the expanding center body diffuser the predicted value is 0.52, which is in excellent agreement with the measured value. This is a surprising result considering the high total pressure loss along the streamline of maximum velocity in this diffuser. The large increase in total pressure loss in the expanding center body diffuser is due to the higher turbulence level of the flow from the inlet bend, increasing the energy dissipation.

In both diffuser systems there is a significant increase in pressure in the downstream settling length—outlet bend. This is due to radial momentum transfer reducing the distortion or momentum coefficient of the velocity profile. In the outlet bend the turbulent mixing normally associated with a grossly distorted velocity profile is accentuated along the outer wall by centrifugal forces.

Mean Velocity Profiles

The development of the mean velocity profiles is shown nondimensionally in Figs. 4 and 5. The profiles exhibited excellent symmetry of flow at all stations, with the exception of the last station in both diffusers where local transitory stalling was observed. The boundary layer parameters are listed in Table 3.

There is a significant difference in growth of the shape parameter H along the inner and outer walls, the value of dH/dx being greater on the outer wall, in fact on the inner wall of the expanding center body diffuser H remains almost constant. The different rates of growth of the shape parameter can be discussed in terms of the mean flow equation. For axisymmetric flow

$$u\frac{\partial u}{\partial x} + v\frac{\partial u}{\partial R} = -\frac{1}{\rho}\frac{\partial P}{\partial x} - \frac{\partial}{\partial x}\langle u'^2\rangle + \left(\frac{\mu}{\rho}\frac{1}{R}\frac{\partial u}{\partial R} - \frac{\langle u'v'\rangle}{R}\right) + \left(\frac{\mu}{\rho}\frac{\partial^2 u}{\partial R^2} - \frac{\partial}{\partial R}\langle u'v'\rangle\right) \qquad (3)$$

If the influence of Reynolds stresses is ignored and the term $v\partial u/\partial R$ is assumed to be small in the inner region of the layer then Eq. (3) reduces to

$$u\partial u/\partial x = -(1/\rho)\partial P/\partial x \qquad (4)$$

In a diffuser where $\partial P/\partial x$ is positive, there will be a reduction in velocity which is inversely proportional to the

Table 3 Boundary-layer parameters

Constant center body diffuser $L/\Delta R_1 = 5.0$								
x/L	−0.60	0.060	0.150	0.270	0.510	0.630	0.750	0.97
α	1.045	1.059	1.089	1.137	1.265	1.346	1.452	1.735
$\bar{u}/U$	0.895	0.885	0.856	0.825	0.756	0.723	0.687	0.612
H_o	1.30	1.39	1.49	1.69	2.12	2.38	2.68	3.52
θ_o in.	0.042	0.046	0.061	0.071	0.099	0.110	0.123	0.138
H_i	1.28	1.31	1.40	1.45	1.57	1.61	1.65	1.69
θ_i in.	0.039	0.044	0.054	0.065	0.086	0.096	0.102	0.115
Expanding center body diffuser $L/\Delta R_2 = 6.2$								
x/L	0	0.089	0.188	0.278	0.376	0.564	0.653	0.841
α	1.054	1.082	1.116	1.141	1.195	1.270	1.300	1.423
$\bar{u}/U$	0.890	0.874	0.852	0.836	0.814	0.792	0.773	0.731
H_o	1.47	1.61	1.77	1.87	2.11	2.40	2.60	2.95
θ_o in.	0.033	0.041	0.048	0.056	0.060	0.069	0.077	0.087
H_i	1.21	1.24	1.26	1.21	1.23	1.26	1.28	1.29
θ_i in.	0.034	0.031	0.033	0.032	0.030	0.029	0.029	0.028

local velocity, and the distortion of the profile and the value of H are increased. This simplified approach is modified by the inclusion of the other terms in the equation, e.g. Reynolds shear stress. In an adverse pressure gradient the shear stress reduces the degree of distortion, and the changes in profile shape will depend on the relative magnitudes of the pressure gradient and Reynolds stress terms. Since the static pressure is nearly constant across any station in the diffuser, the boundary layers on inner and outer walls must experience the same pressure gradient and therefore the asymmetric growth of the shape parameters is due to: 1) initial distortion produced by the flow curvature at entry, and/or 2) significantly different turbulence structures in the inner and outer wall layers.

Whereas the inlet flow turning angle on the outer wall of the uniform center body diffuser is considerably less than that in the expanding center body diffuser, in both cases the static pressure distributions shown in Fig. 3 indicate that after the minimum pressure point the boundary layer on the outer wall experiences a more severe adverse pressure gradient. This is reflected in a higher shape parameter on the outer wall at the station $x/L = 0.04$ just downstream of the disturbance associated with the flow curvature at inlet, $H_o = 1.37$, $H_i = 1.30$ in the uniform center body diffuser, and $H_o = 1.49$, $H_i = 1.22$ in the expanding center body diffuser. Whereas the turbulence structure of the flow at inlet to the two diffusers is quite different, analysis of the data[6] indicates that the Reynolds stress term in the mean flow equation is small in comparison with the pressure gradient term. Under such conditions Coles[8] has suggested that the mean motion is determined by the pressure forces alone. Therefore in both diffusers the asymmetric growth of the shape parameters is attributed to the initial distortion caused by flow curvature at inlet which is then accentuated by the severe adverse pressure gradient. The slightly higher value of exit outer wall shape parameter obtained in the uniform center body diffuser is considered to be due to the larger pressure gradient, whereas the almost constant inner wall shape parameter in the expanding center body diffuser is thought to be due to the much higher initial level of turbulent mixing offsetting the influence of the pressure gradient.

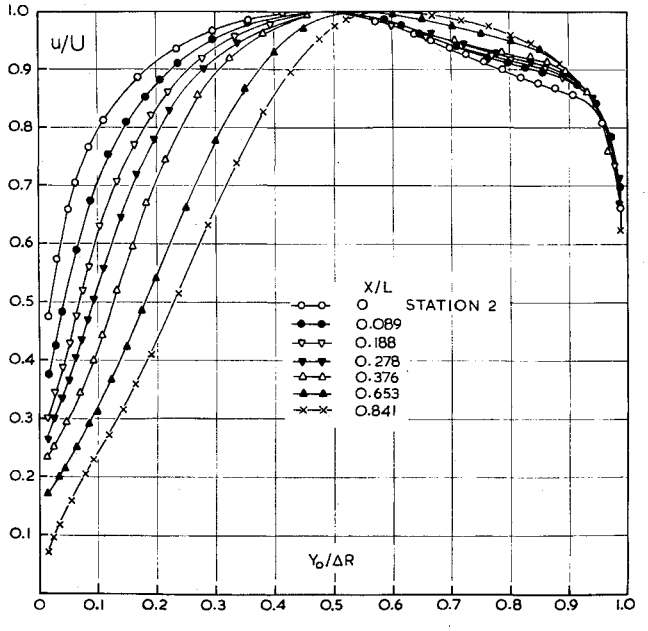

Fig. 5 Velocity profiles along the $L/\Delta R_2 = 6.2$ diffuser.

Shear Stress Distribution

The distribution of turbulent shear stress at one circumferential position is shown in Figs. 6 and 7. At a number of stations measurements were made of the shear stress distribution at three circumferential positions, 120° apart, within the limits of experimental error the distributions are symmetrical. The data shows that in an adverse pressure gradient the value of $-2\langle u'v'\rangle/U^2$ near the wall develops to a maximum which increases and moves away from the wall as the flow proceeds downstream.

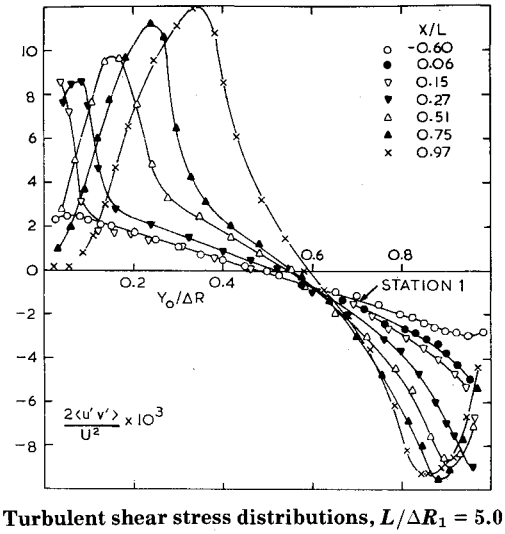

Fig. 6 Turbulent shear stress distributions, $L/\Delta R_1 = 5.0$ diffuser.

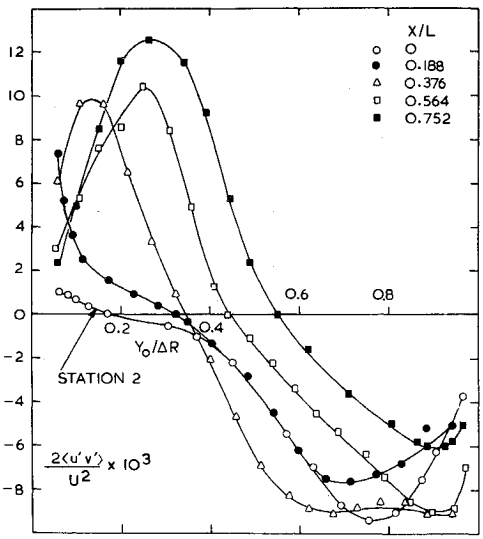

Fig. 7 Turbulent shear stress distributions, $L/\Delta R_2 = 6.2$ diffuser.

The steep gradients of shear stress normal to the walls of the diffusers can be explained by writing the mean flow Eq. (3) near the wall as

$$dP/dx = d\tau/dy \text{ where } \tau = \langle -\rho u'v' \rangle + \mu(\partial u/\partial R) \quad (5)$$

The two-dimensional version has been used in view of the large hub/tip ratio. Therefore in the initial stages of diffusion where the pressure gradient is at its maximum value steep gradients of shear stress are observed near the wall. A number of workers, notably Spangenberg et al[12] have investigated the validity of Eq. (5). Spangenberg et al, in an investigation of a near separating layer found that at no point near the wall did $d\tau/dy$ equal dP/dx, in fact close to separation $d\tau/dy \simeq 0.2dP/dx$. As separation was approached a condition of near zero wall shear stress was reached and in this region the force required to overcome the pressure gradient was found to be derived mainly from the Reynolds normal stresses, a value $d\langle u'^2\rangle/dx \simeq 0.6dP/dx$ being obtained near to separation.

Examination of the data along the outer wall of the uniform center body diffuser revealed that $d\tau/dy \simeq 0.8dP/dx$ in the initial stages of diffusion, falling to $d\tau/dy \simeq 0.25dP/dx$ at $x/L = 0.75$. The gradient of Reynolds normal stresses near the wall at this point was found to be equal to approximately $0.3dP/dx$. It appears therefore that at this point the other terms in the mean flow equation must be taken into account.

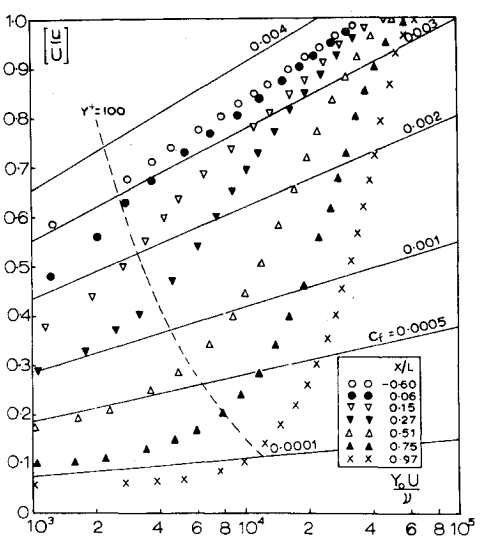

Fig. 8 Clauser plot of velocity profiles, $L/\Delta R_1 = 5.0$ diffuser.

Skin-Friction Coefficients

No direct measurements were made of wall shear stress, and the skin friction coefficient was estimated from the measured velocity profiles using the method due to Clauser.[13] The "law of the wall" is replotted in Fig. 8 as a universal family for a range of values of C_f. It can be seen that there is an absence of any clear logarithmic portion in most of the measured profiles, even down to values of yu_τ/ν as low as 100, and under these circumstances the values of C_f can only be considered as approximate. The conventional form of the law of the wall may be obtained using Prandtl's assumption that the shear stress outside the laminar sublayer may be written as

$$\tau = \rho k^2 y^2 (du/dy)^2 \quad (6)$$

and that the shear stress τ remains constant at the wall value (τ_w). Integration of Equation (6) yields

$$u = (1/k)(\tau_w/\rho)^{1/2} \log_e y + \text{const} \quad (7)$$

Equation (7) has been found to be valid not only in the vicinity of the wall, but over a much larger proportion of the layer than would normally be expected. Although the pressure gradients in Ludwieg and Tillmann's[14] experiments were relatively small, their results have often been used to justify the assumption that Eq. (7) holds in an adverse pressure gradient. However when the boundary layer is subjected to a severe pressure gradient it has been shown that there is a large gradient of shear stress normal to the wall, and therefore the constant shear stress hypothesis is invalidated. Townsend[15] has considered the influence of a shear stress gradient, writing

$$\tau = \tau_\omega + (dP/dx)y = \rho k^2 y^2 (du/dy)^2$$

which integrates to give

$$\frac{u}{u_\tau} = \frac{2}{k}[(\gamma y^+ + 1)^{0.5} - 1] + \frac{1}{k} \log_e \left[\frac{4}{\gamma} \frac{(\gamma y^+ + 1)^{0.5} - 1}{(\gamma y^+ + 1)^{0.5} + 1}\right] + B^+ \quad (8)$$

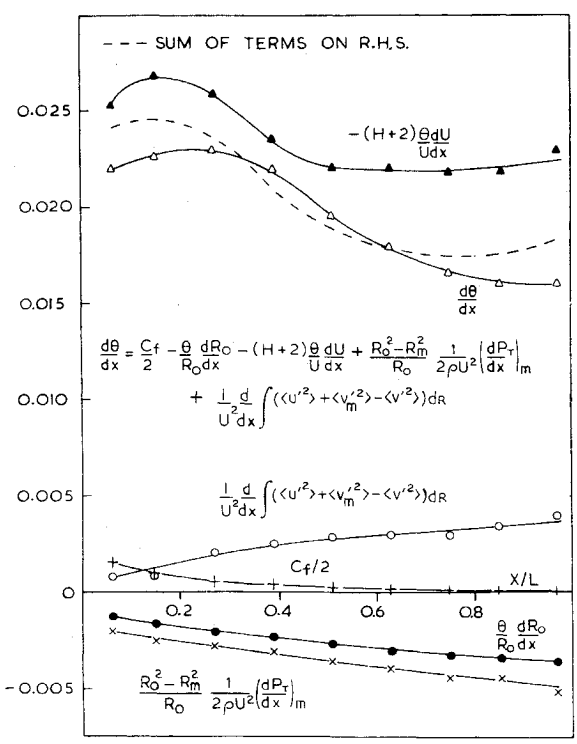

Fig. 9 Balance of momentum integral equation, outer wall, $L/\Delta R_1 = 5.0$ diffuser.

where $\gamma = (\nu/\rho u_\tau^3)(dp/dx)$ is the ratio of pressure to viscous forces, $y^+ = yu_\tau/\nu$, $B^+ = 5.0$, and $k = 0.4$.

The correctness of the "conventional" universal equation is therefore seen to depend on the magnitude of the parameter γ. The "strong adverse pressure gradient" data of Ludwieg and Tillmann corresponds only to values of $\gamma \leq 0.0035$, and Thompson[16] has indicated that departures from the universal law will occur for $\gamma > 0.10$. The experimental values of γ, for the uniform center body diffuser are given in Table 4.

It can be seen that the values of γ are very much greater than those recorded in Ludwieg and Tillmann's experiments, and the failure of the profiles to exhibit a logarithmic variation near the wall is attributed to the severe adverse pressure gradient.

Momentum Balance Plots

As a guide to the accuracy of the experimental data and the relative significance of the terms in the momentum integral equation, momentum balances were carried out at a number of stations along the length of the diffuser. Writing the momentum equation for the flow along the outer wall as

$$\frac{d\theta_0}{dx} = \frac{C_{f_o}}{2} - \frac{\theta_o}{R_0}\frac{dR_0}{dx} - \frac{\theta_o}{U}\frac{dU}{dx}(H_o + 2) + \frac{R_0^2 - R_m^2}{R_0}\frac{1}{2\rho U^2}\left(\frac{dP_T}{dx}\right)_m + \frac{1}{U^2}\frac{d}{dx}\int_0^{\delta_o}(\langle u'^2\rangle + \langle v_m'^2\rangle - \langle v'^2\rangle)\frac{R}{R_o}dR \quad (9)$$

If a potential core exists at a station in the diffuser, then at that station, $(dP_T/dx)_m = 0$ and $d(\langle v_m'^2\rangle)/dx = 0$ also in view of the large radius ratio the two-dimensional form of the Reynolds normal stress term has been adopted viz.

$$1/U^2 d/dx \int_0^{\delta_o}(\langle u'^2\rangle + \langle v_m'^2\rangle - \langle v'^2\rangle)dy \quad (10)$$

The experimental values of θ, H, U, R_m, etc., have been used to calculate the terms on the right-hand side of the equation, and the predicted value of $d\theta/dx$ is compared in Fig. 9 with the value estimated from the gradient of the measured values of momentum thickness. Discrepancies in the values of θ are frequently attributed to three-dimensional effects, and Coles[8] has found that a balance is rare in flows developed in a strong adverse pressure gradient. It can be seen that in all cases the comparison between the left and right-hand sides of the equation is very good. In view of this, and bearing in mind the symmetry of the mean velocity profiles, and the good agreement in integrated mass flows, it can be stated that the data is free from any significant three-dimensional effects. This is thought to be due to the choice of an annular configuration in which the center body has a stabilising effect, and the high standard of accuracy maintained throughout the construction of the rig. The main conclusions to be drawn from the momentum-balance results are: 1) Apart from the initial stages of diffusion the skin friction term is extremely small. 2) The contribution due to Reynolds normal stresses is of comparable magnitude to the transverse curvature term. 3) The term incorporating the pressure gradient $(H + 2)(\theta/U)dU/dx$ dominates the equation. However the term incorporating the gradient of total pressure along the streamline of maximum velocity $[(R_0^2 - R_m^2)/R_0]_1/(2pU^2)(dP_T/dx)_m$ is also siginificant. This is particularly so in the case of the expanding center body diffuser where an increased loss in stagnation pressure is experienced on account of the intensified turbulent mixing presented by the inlet bend.

Table 4 Approximate values of γ

Constant center body diffuser $L/\Delta R_1 = 5.0$							
x/L	0.150	0.270	0.390	0.510	0.630	0.750	0.856
γ_o	0.055	0.093	0.156	0.197	0.364	0.665	1.460
γ_i	0.043	0.043	0.038	0.038	0.036	0.031	0.028

Conclusions

Whereas the static pressure recovery of the two diffuser systems is comparable there is a significant difference in the loss of mean total pressure. The loss in the expanding center body diffuser is much greater and is attributed to the increased turbulent mixing in the flow after the inlet bend. In the same context, although the dynamic pressures are lower, the losses in the outlet bend are larger than would be normally expected. However in this case turbulent mixing reduces the distortion of the velocity profile resulting in a significant recovery of static pressure.

A detailed investigation of the growth of the boundary layers in two optimum diffusers suggests that: 1) In the initial stages of diffusion, downstream of the disturbance due to the inlet bend, the flow is dominated by pressure forces. 2) The disturbance associated with the curvature of flow at inlet presents the diffuser with a distorted inlet velocity profile which is accentuated by the pressure gradient. The asymmetry associated with the distorted inlet conditions leads to a much larger rate of growth of the shape parameters along the outer wall. 3) Due to the large gradient of shear stress normal to the wall, the conventional form of the "law of the wall" equation ceases to be valid in a strongly retarded flow. 4) The turbulent shear stress distribution lags behind the development of the mean velocity profile, furthermore in the expanding center body diffuser there is a considerable difference between the positions of zero shear stress and maximum velocity.

References

[1]Kline, S. J., Abbott, D. E., and Fox, R. W., "Optimum Design of Straight-Walled Diffusers," *Transactions of the ASME, Journal of Basic Engineering*, Vol. 81, 1959, pp. 321—329.

[2]Sovran, G. and Klomp, E. D., "Experimentally Determined Optimum Geometries for Rectilinear Diffusers with Rectangular, Conical, or Annular Cross-Section," *Fluid Mechanics of Internal Flow*, Elsevier, New York, 1967, pp. 270–319.

[3]Hoadley, D., "Three-Dimensional Turbulent Boundary Layers in an Annular Diffuser," Ph.D. thesis, 1970, Mechanical Engineering Dept., University of Cambridge, Cambridge, England.

[4]Cocanower, A. B., Kline, S. J., and Johnston, J. P., "A Unified Method for Predicting the Performance of Subsonic Diffusers of Several Geometries," Rept. PD-10, Mechanical Engineering Dept., Stanford University, 1965, Stanford, Calif.

[5]Imbach, H. E., "Calculation of Rotationally Symmetrical Turbulent Flow Through Diffusers," *The Brown Boveri Review*, Vol. 51, No. 12, 1964, pp. 789–801.

[6]Stevens, S. J., "Turbulent Incompressible Flow in Annular Diffusers," Ph.D. thesis, 1970, Dept. of Transport Technology, University of Technology, Loughborough, England.

[7]Girerd, H. and Guienne, P., "Nouvelles Sordes de Pression Statique pour Mesures Aerodynamiques," *Compte rendu Acadamie Scientifiques*, Vol. 228, July 1949, pp. 651—653.

[8]Coles, D., "The Young Person's Guide to the Data," *Proceedings Computation of Turbulent Boundary Layers—1968 AFOSR-IFP-Stanford Conference*, Vol. 2, Stanford University Press, 1968, Stanford, Calif.

[9]Goldberg, P. M., "Upstream History and Apparent Stress in Turbulent Boundary Layers," Gas Turbine LR-85, 1966, Massachusetts Institute of Technology, Cambridge, Mass.

[10]Sandborn, V. A. and Liu, C. Y., "On Turbulent Boundary Layer Separation," *Journal of Fluid Mechanics*, Vol. 32, May 1968, pp. 293—304.

[11]Wattendorf, F., "Study of the Effect of Curvature on Fully Developed Turbulent Flow," *Proceedings of The Royal Society*, Vol. A148, 1935, pp. 568–598.

[12]Spangenberg, W. G., Rowland, W. R., and Mease, N. E., "Measurements in a Turbulent Boundary Layer Maintained in a Nearly Separated Condition," *Fluid Mechanics of Internal Flow*, Elsevier, New York, 1967, pp. 110–151.

[13]Clauser, F. H., "Turbulent Boundary Layers in Adverse Pressure Gradients," *Journal of Aeronautical Sciences*, Vol. 21, Feb. 1954, pp. 91–108.

[14]Ludwieg, H. and Tillmann, W., "Investigations of the Wall Shearing Stress in Turbulent Boundary Layers," TM 1285, 1950, NACA.

[15]Townsend, A. E., "The Behaviour of a Turbulent Boundary Layer near Separation," *Journal of Fluid Mechanics*, Vol. 12, April 1962, pp. 536–554.

[16]Thompson, B. G. J., "A New Two-Parameter Family of Mean Velocity Profiles for Incompressible Turbulent Boundary Layers on Smooth Walls," R&M 3463, 1967, Aeronautical Research Council, London, England.

Dynamics of Slung Bodies Using a Single-Point Suspension System

Corrado Poli* and Duane Cromack†
University of Massachusetts, Amherst, Mass.

A stability analysis of slung bodies of current, practical interest, and the identification of the towing system parameters which affect stability is presented. The analysis is accomplished by first determining the aerodynamic characteristics of two nonstreamlined bodies; an 8 ft × 8 ft × 20 ft cargo container, and a 20-ft-long, 5.4-ft-diam right-circular cylinder. These results are then used in a linearized small-perturbation stability analysis of the slung system. For the single-point system, it is shown that long cables, high speeds, and light loads are required for stability. The drag-to-weight ratio of the towed body and the length of the cable are shown to be the most important stability parameters.

Nomenclature

a,h = horizontal and vertical distances between attachment points
A,B,C = moments of inertia of the towed body about the x,y,z axes
D/W = drag-to-weight ratio
d_1,d_2 = distance from c.g. of slung load to the attachment point, measured in the XYZ system (primed quantities are measured in xyz system)
l = cable length
L,M,N = aerodynamic moments
m = mass of the towed body
r/w = edge radius-to-body width ratio
T_o = steady-state cable force
u,v,w = linear perturbation
U_o = steady-state velocity
X,Y,Z = aerodynamic forces
θ,ψ,ϕ = aircraft Euler angles
α = angle of attack
β = side-slip angle
γ = steady-state tow angle (Fig. 3)
C_D = drag coefficient
C_L = lift coefficient
C_Y = side-force coefficient
C_l = roll moment coefficient (moment measured about c.g.)
C_m = pitch moment coefficient (moment measured about c.g.)
C_n = yaw moment coefficient (moment measured about c.g.)
$C_{L\alpha}$ = $\partial C_L/\partial\alpha$
$C_{m\alpha}$ = $\partial C_m/\partial\alpha$
$C_{y\beta}$ = $\partial C_y/\partial\beta$
C_{n_β} = $\partial C_n/\partial\beta$
X_u,X_w, etc. = changes in the aerodynamic forces and moments due to changes in velocity
Re = Reynolds Number

Received June 15, 1972; presented as Paper 72-986 at the AIAA 2nd Atmospheric Flight Mechanics Conference, Palo Alto, Calif., September 11–13, 1972; revision received November 1, 1972. This work was supported by the U.S. Army Research Office—Durham.

Index category: VTOL Handling, Stability, and Control.

*Professor, Mechanical and Aerospace Engineering Department. Member AIAA.

†Associate Professor, Mechanical and Aerospace Engineering Department. Member AIAA.

Introduction

IN 1930, Glauert[1] performed what appears to be the first comprehensive study into the dynamics of towed bodies when he investigated the lateral and longitudinal stability of a nonlifting body towed by a light inextensible wire. While additional valuable work has been done in the area of airborne towing[2-15] (Ref. 12 should be consulted for a comprehensive survey), a study of the available literature shows that few quantitative results are available for the dynamic state during the towing of nonaerodynamic shaped bodies, such as a palletized cargo, beneath rotary winged aircraft.

The increased importance of towing becomes clear when one begins to imagine conditions when it would become desirable to transport some heavy operational equipment from one remote and inaccessible area of operation to another, or even from sea to land. One way, and in some cases possibly the only way, to perform quickly this transportation of equipment would be to have a helicopter tow the gear from one region to another. It is also conceivable that towing of cargo could greatly reduce the costly delays in overseas shipping schedules often caused by inadequate or nonexistent port facilities in remote and underdeveloped areas where vessels could stand idle for weeks before their cargo can be unloaded. In such situations if the airlifting of equipment is to be performed successfully, then the towing must be accomplished with a minimum amount of unstable motion. Hence, before a system can be considered operational, it is necessary to establish the ranges of operation in which instabilities are likely to occur.

The need for such investigations is quite clear. For instance, Etkin and Macworth[5] report of the serious instability which occurred when attempts were made to tow